EE

LABORATORI NAZIONALI DI FRASCATI
SIS – Pubblicazioni

LNF-94/053 (IR)
26 Settembre 1994

Source Size and Brilliance of Infrared Radiation Emitted by a Bending Magnet of DAΦNE

A. Nucara, P. Calvani
Universitá La Sapienza, Dipartimento di Fisica, P.le A. Moro 1, 00100 Roma, Italy

A. Marcelli
I.N.F.N. - Laboratori Nazionali di Frascati, Casella Postale 13, 00044 Frascati, Italy

M. Sànchez del Rio
European Synchrotron Radiation Facility, B.P. 220, 38043 Grenoble-CEDEX, France

Abstract

The Actual Source Area (ASA) of a bending magnet in the infrared range, has been calculated for the Φ-factory DAΦNE under construction at Frascati. "Geometrical" broadening has been included.
The Actual Brilliance Ratio (ABR) defined as the ratio between the brilliance of a synchrotron source and that of a blackbody, has been also evaluated for DAΦNE and compared with the Brookhaven NSLS source.

PACS.: 41.60.Ap; 41.85.Le; 07.65.Gj

Introduction

The synchrotron radiation emitted in large fan by a bending magnet (BM) is usually collected within a small horizontal angle θ ranging from 5 to 10 mrad. This angle corresponds to an orbit of a few mm length for a typical magnet radius of a few meters. Longer portions of orbit subtend larger angles, up to 50 or 100 mrad. Synchrotron radiation (SR) from these large angles could be in principle collected by using optical surfaces, i.e., mirrors or multilayers. However, the main obstacle, in particular in the x-ray range by using reflecting optics at grazing incidence, is the need of very long optical elements and/or aspherical surface shapes. Moreover for large collecting angles the broadening of the source is considerable and the aberrations introduced by optics make the image in the focus point large and asymmetric. These effects are very large in the x-ray range but are present in the vacuum ultraviolet (VUV) and in the infrared region (IR) too. In the following we will illustrate a calculation of the Actual Source Area (ASA) for the IR energy range. The estimate of the source size is a first step to obtain the Actual Brilliance Ratio (ABR), defined as the gain of a storage ring, with respect to either a black body or a Globar source.

Synchrotron radiation is a non-thermal radiation characterized by a high degree of polarization.[1] SR bending magnet sources reach high linear polarization rate (>90%) in the plane of the ring. Moreover, special insertion devices producing intense and bright vertically, or circularly polarized beams can be installed in a storage ring.

We can start defining the brilliance of the SR source as

$$B = \left(\frac{dF}{d\theta d\varphi dx dy} \right) \qquad \text{photons/rad}^2\text{/s/cm}^2 \qquad (1)$$

In Eq. 1 F is the flux of photons emitted by the particles along their trajectory, dθ and dφ are the horizontal and vertical emission angles, x and y the horizontal and vertical coordinates, respectively. Taking into account the natural broadening of the SR source, we may better define the brilliance such as the flux F emitted in the solid angle dθdφ, by the ASA. Here, Σ_x and Σ_y are the r.m.s. values of the horizontal and vertical dimensions of the source, and $2\pi\Sigma_x\Sigma_y$ is the area, which approximates an extended source. The brilliance then becomes:

$$B = \left(\frac{dF}{d\theta d\varphi (2\pi\ \Sigma_x \Sigma_y)} \right) \qquad \text{photons/rad}^2\text{/s/cm}^2 \qquad (2)$$

An expression for the ASA which takes into account physical effects and ring parameters associated with the dynamics of the electron beam, can be found for example in Ref. 2. Nevertheless, one should add to such formula the contributions σ_i^{geo} ("*geometrical broadening*"), which are due to the finite length of the particle trajectory in the bending magnet. One finds out:

$$ASA = 2\pi\Sigma_x\Sigma_y = 2\pi \sqrt{\sigma_x^2+\sigma_r^2+\left(\sigma_x^{geo}\right)^2}\ \sqrt{\sigma_y^2+\sigma_r^2+\left(\sigma_y^{geo}\right)^2} \qquad (3)$$

In Eq. 3, σ_x and σ_y are the horizontal and vertical size due to the electron beam size as well as to the optical functions of the ring, while σ_r is the diffraction-limited source size.

Equation 3 includes also the terms σ^{geo}_x and σ^{geo}_y due to the collection of a finite length of trajectory along a bending magnet of radius ρ.

In the following sections the different contributions to ASA will be discussed. Then this theoretical prediction will be compared with ray-tracing simulation. At the end a comparison among several BM infrared sources will be presented.

A. The source size σ_x, σ_y

To calculate the beam dimensions σ_i (i = x, y) and the divergences σ'_i we can use the standard equations, which contain the emittances ε_i and the dispersions β_i.[3] The theoretical σ_x is given by:

$$\sigma_x = \sqrt{\sigma_{0x}^2+\sigma_{Mx}^2} = \sqrt{\varepsilon_x\beta_x+(\eta_x\sigma_\varepsilon)^2} \qquad (4)$$

In Eq. 4, $\sigma_{0x} = \sqrt{\varepsilon_x\beta_x}$ is the electron beam dimension and the additional horizontal broadening σ_{Mx} is due to the dispersion function η_x in the x location at the BM and to the relative r.m.s. energy-spread σ_ε in the anomalous bunch lengthening regime. The term σ_{0x} in Eq. 4 is usually the most relevant contribution to the horizontal size. Similarly, the vertical value σ_y is given by two contributions:

$$\sigma_y = \sqrt{\sigma_{0y}^2+\sigma_{My}^2} = \sqrt{\varepsilon_y\beta_y + \frac{\varepsilon_y^2 + \varepsilon_y\gamma_y\sigma_r^2}{\sigma_\psi^2}} \qquad (5)$$

where $\sigma_{0y} = \sqrt{\varepsilon_y\beta_y}$,and σ_{My} depends by the third betatron function γ_y in the y direction, defined as $\gamma_y=(1+\alpha_y^2)/\beta_y$ and by σ_r and σ_ψ.[4]

By using the above equations and the parameter reported in Refs. 5, 6 we can calculate the beam dimensions for the bending magnet source of DAΦNE as well as for several IRSR sources (see **Table** I). The vertical contribution σ_{My} from the optical functions of the machine is calculated for λ=50 μm, and it results much smaller then σ_{0y}. However, it may become comparable with σ_{0y} at higher wavelength.

TABLE I – Parameter and estimated values of source size of synchrotron radiation facilities. The values σ_{Mi} are calculated for λ=50 μm.

BM	E (GeV)	ε_x 10^{-6} (cm rad)	ε_y 10^{-6} (cm rad)	σ_x (cm)	σ_y (cm)	σ_{Mx} (cm)	σ_{My} 10^{-5} (cm)
DAΦNE[a]	0.51	100	1	0.217	0.031	0.0198	3.2
MAX I[b]	0.55	3	0.48	0.049	0.02	0.0045	
NSLS[c]	0.745	13.8	0.4	0.058	0.0197	0.045	1.4
UVSOR[d]	0.75	3.66	0.366	0.039	0.027		
SuperACO[e]	0.80	3.7	1.8	0.038	0.030	0.064	5.2

[a]Ref. 5
[b]MAX-LAB Activity Report 1990
[c]Ref. 2
[d]UVSOR Activity Report 1993
[e]P. Roy, private commun.

B. The diffraction-limited size σ_r

A source point emitting at the wavelength λ in the collecting angle θ, has a minimum dimension given simply by

$$\sigma_r = \frac{\lambda}{4\pi\theta} \tag{6}$$

This r.m.s. value corresponds to the radius of a circular slit which would diffract the radiation at the wavelength λ. In the case of SR the solid angle θ in the infrared spectral region corresponds to

$$\sigma_\psi(\lambda) = 0.816 \left(\frac{\lambda}{\lambda_c}\right)^{0.354} \frac{10^{-3}}{E(GeV)} \qquad \text{(rad)} \tag{7}$$

In the above relation the exponent of the (λ/λ_c) ratio has been derived in the limit $\lambda/\lambda_c >> 1$, i.e. for the IR range.[7] However, because σ_ψ is a complicate function of the (λ/λ_c) ratio, different asymptotic expressions in the IR range are reported in the literature with similar behavior.[8,9]

The diffraction limited size of a point source in a BM can thus be found by replacing in Eq. (6) the collecting angle θ with the above definition for the intrinsic divergence of the radiation

$$\sigma_r(\lambda) = \frac{\lambda}{4\pi\sigma_\psi(\lambda)} \tag{8}$$

C. The horizontal and vertical geometrical broadenings σ^{geo}_x and σ^{geo}_y

When collecting under small angles the geometrical terms are usually neglected in the x ray and soft x ray range. This is not the case of the IR radiation, because of the simultaneous effect of the large intrinsic spread σ_ψ and of the large collecting angle θ. When this angle is increased, the SR source becomes an arc of length $2\theta\rho$ where ρ is the radius of the BM. The geometrical terms here introduced represent the projection of the source arc of length l, on the xy plane intersecting the arc length at its mid-point. Such projection is assumed as the virtual location of the extended source. The term σ^{geo}_y describes the contribution to the vertical dimension and it is associated with the opening angle of the radiation σ_ψ.

A first attempt to estimate the horizontal broadening Δ of a source has been made by Williams.[9] Moreover, calculations extended to insertion device sources, as undulators and wigglers, are discussed by Skrinsky.[10] In Fig. 1 is showed the broadening Δ as a function of θ, for ρ=191 cm (NSLS) and ρ=140 cm (DAΦNE). This function is calculated by using the expression:

$$\Delta = \rho(1 - \cos\theta/2) \tag{9}$$

However, Δ in Eq. (9) represents the total horizontal extension of the source and it results to be larger then the r.m.s. value σ^{geo}_x. This latter can be estimated by using a statistical distribution for the source points. One has

$$(\sigma_x^{geo})^2 = \langle x^2 \rangle - \langle x \rangle^2 = \frac{3}{2}\rho^2 + \frac{1}{2}\rho^2 \frac{\sin\theta}{\theta} - 2\rho^2 \frac{\sin\theta/2}{\theta/2} - \rho^2 \left(1 - \frac{\sin\theta/2}{\theta/2}\right)^2 \qquad (10)$$

A similar statistical approach is applied for the vertical, where however are taken into account the different role of the geometry in the vertical direction and the contribution of the intrinsic divergence of the synchrotron radiation, that yields to the expression

$$(\sigma_y^{geo})^2 = \langle y^2 \rangle = \frac{\rho^2 \tan^2(\sigma_{\nu}/2)}{2\theta} [\sin^2(\theta/2)\tan(\theta/2) - \theta + 2\sin(\theta/2)] \qquad (11)$$

Details of the calculations are reported in the Appendix.

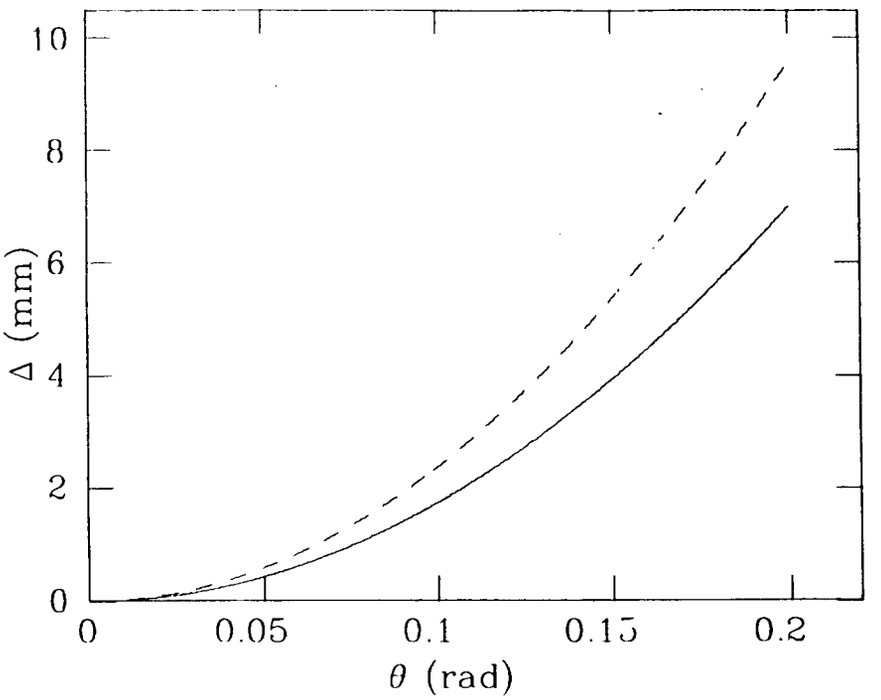

FIG. 1 – The increase of the horizontal size Δ (Eq. 9 in the text) as a function of the collecting angle θ. The solid line refers a DAΦNE BM, the dashed line to a NSLS BM.

D. Comparison with ray-tracing simulation

The terms above introduced are the elements to obtain an estimate of ASA. The values of $\sigma^{geo}{}_x$ and $\sigma^{geo}{}_y$ once calculated can be compared, for different IR wavelengths, with the size of the source generated by a ray tracing. The DAΦNE bending magnet source has been simulated by ray-tracing, starting from the ring parameters[5] reported in Table II. The corresponding NSLS input data[6] are also reported in the same Table.

TABLE II – Parameters used for the ray tracing calculation.

	E (GeV)	λ_c (μm)10^{-4}	σ_x (mm)	σ_y (mm)	θ (mrad)	ρ (cm)
DAΦNE	0.51	59.6	2.17	0.313	50	140
NSLS	0.745	25.5	0.58	0.197	50	191

The results of the simulation are shown in Table III. Here, the values of the simulated source size σ_x^{sim} and σ_y^{sim} include both σ_i and the geometrical contributions, then they have to be compared only with the corresponding calculated values $\sqrt{\sigma_i^2 + (\sigma_i^{geo})^2}$ excluding σ_r. The simulation of the NSLS source listed in Table III, yields to a geometrical broadening σ^{geo}_x=0.157 mm (not reported in the table), a value very similar to σ^{geo}_x=0.177 mm calculated from Eq. 10. Moreover, in the case of the NSLS source, also the average displacement <x> = 0.2 mm can be extracted and its value is in good agreement with the calculated one (see Eq. A3). For DAΦNE the estimate of the horizontal geometrical broadening indicates σ^{geo}_x=0.370 mm, a value larger than the one calculated. Indeed, in the case of DAΦNE, for a collection angle of 50 mrad the large horizontal source size due to the beam masks any other effect and the horizontal geometrical broadening as well as the average <x> are negligible. On the contrary, in the case of NSLS both beam size and geometrical horizontal broadening are of the same order of magnitude. In fact, for the vertical case, Table III shows that the values of σ_y^{sim} are very similar to those obtained from Eq. 11 for both DAΦNE and NSLS.

E. The diffraction limit of the SR source.

The diffraction limited size given by Eq. 8 is just the lower size of a single point source and its calculation do not consider the geometrical constraints associated with the acceptance of a limited solid angle. Actually, if we consider the extended source as a surface placed in the middle of the curved electron trajectory, we see that the source is intrinsically limited by diffraction. The effect is associated with the angular distribution $\sigma_\psi(\lambda)$ and with the geometrical constraint of the collecting system. At the first optical element (i.e., mirror, slit, window) the source is seen under an horizontal angle θ and a vertical angle determinated by $\sigma_\psi(\lambda)$, so that radiation is collected within an actual solid angle

$$\Omega = \theta\sigma_\psi(\lambda) \tag{12}$$

Equation 12 results in an increase of the ASA by a factor

$$\sigma_{LD}^2 = \frac{\lambda^2}{(4\pi)^2\Omega} \tag{13}$$

TABLE III – Parameter and estimated values of source size of synchrotron radiation facilities. The values σ_{Mi} are calculated for λ=50 μm.

	<x> (mm)	σgeo_x (mm)	σ_y^{geo} (mm)				σ_r (mm)				σ_x^{sim} (mm)	σ_y^{sim} (mm)			
			λ=10	λ=100	λ=1000	λ=5000	λ=10	λ=100	λ=1000	λ=5000		λ=10	λ=100	λ=1000	λ=5000
NSLS	0.199	0.177	0.198	0.45	1.02	1.81	0.039	0.172	0.761	2.15	0.601	0.198	0.37	0.732	1.23
DAΦNE	0.146	0.130	0.158	0.357	0.808	1.433	0.036	0.159	0.703	1.99	2.202	0.352	0.462	0.739	1.089

This r.m.s. value corresponds to the area of a slit which diffracts the radiation at the wavelength λ and represents a lower limit for the ASA. Starting from these considerations, to understand the effect of the diffraction limit to the total source area it is useful to plot the function $D(\lambda) = 2\pi\Sigma_x\Sigma_y\Omega + \lambda^2$ vs. λ (**Fig. 2**). For wavelengths much smaller than the ASA (λ<1μm), the area-solid angle product is almost independent of λ. In this case the function exhibits a λ dependence with a simple power law, as expected for a simple dependence by σ_ψ. On the contrary, at wavelength of the same order of the ASA (λ~1 mm) the diffraction limit is effective and at very large λ (cm range) it becomes the most important contribution. In Fig. 2 the area-solid angle product is plotted for the DAΦNE source for collecting angles of 20 and 50 mrad. For λ>3 x10^3 μm, values that approximate the ASA of DAΦNE, the dependence on λ is a power law with exponent equal to 2, as expected for a fully diffracted source.
Further effects associated with the interference of light may also modify the spectral angular distribution of SR in the far IR range as discussed in Ref. 11.

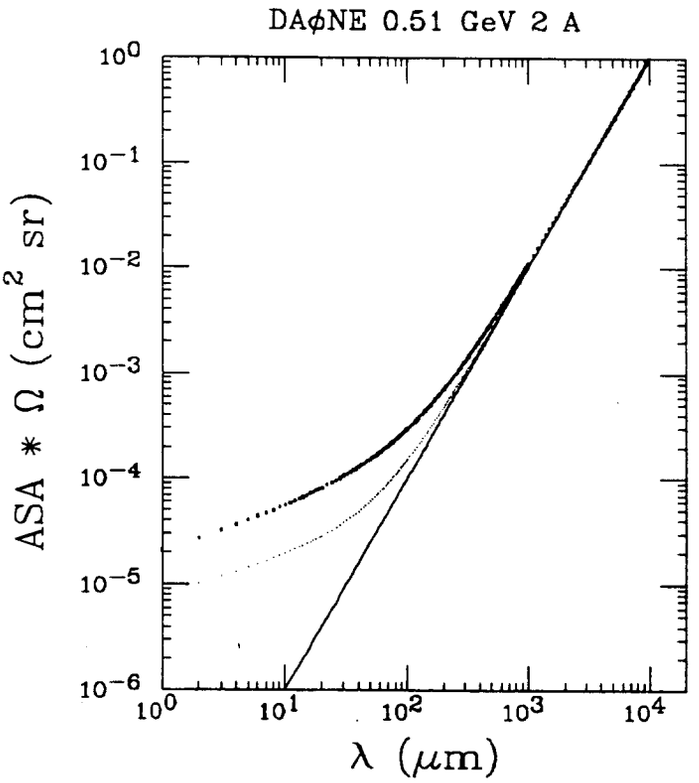

FIG. 2 – Plot of the area-solid angle product for the DAΦNE source. The curves are for collecting angles of 20 mrad (dots) and 50 mrad (dashes). The solid line represents a fully diffracted source.

F. The Actual Brilliance Ratio

The advantage of using synchrotron radiation in the infrared region lies in its high brilliance. A comparison with conventional sources like a black body (BB) or a Globar can be obtained by defining the Actual Brilliance Ratio (ABR) as the ratio between the brilliance of the synchrotron source and the brilliance of a blackbody.
The brilliance of the SR source given by Eq. 2 becomes[2]

$$B_{SR} = \frac{\left.\frac{d^2F}{d\theta d\varphi}\right|_{\varphi=0}}{ASA(cm^2)} \qquad \text{photons/0.1\%bw/s/cm}^2\text{/str} \qquad (14)$$

where

$$\frac{d^2F}{d\theta d\varphi} = 1.327\ 10^{19}\ E^2(GeV)\ I(A) \left(\frac{\lambda_c}{\lambda}\right)^2 K_{2/3}^2 \left(\frac{\lambda_c}{2\lambda}\right). \qquad (15)$$

is the flux of photons in the solid angle for a bandwidth $\Delta\nu=0.001\nu$. The modified Bessel function in Eq. 15 may be evaluated by using the rule given in Ref. 12

$$K_{2/3}(x) = 1.81380\ (0.592542\ x^{-2/3} - 0.697828\ x^{2/3}) \qquad (16)$$

where $x=\lambda_c/2\lambda$, valid in the limit $x<0.002$.[13] In the case of the DAΦNE source, being λ_c=59.6 Å, this relation is verified for $\lambda \geq 1.5$ μm. The brilliance of a blackbody source can be derived starting from the well known Planck's law for the power density.[14] Indeed, the brilliance $B_{BB}(\nu,T)$ of the blackbody is related to the specific energy density by the relation

$$B_{BB}(\nu,T) = \frac{2}{c^2}\frac{h\nu^3}{(e^{\beta h\nu}-1)}d\nu \qquad \text{erg/s/cm}^2\text{/str} \qquad (17)$$

To obtain the brilliance we may divide the black body brilliance of Eq. 17 by the photon energy $h\nu$, select a finite bandwidth $\Delta\nu=0.001\nu$, and put $\lambda=c/\nu$:

$$B_{BB}(\lambda,T) = \frac{2}{\lambda^3}\frac{0.001c}{(e^{\beta hc/\lambda}-1)} \qquad \text{photons/0.1\%bw/s/cm}^2\text{/str} \qquad (18)$$

We can now calculate the function ABR considering a blackbody source at T=2000 K. The results are shown in Fig. 3 for DAΦNE and in Fig. 4 for NSLS. Both figures show the advantage of the SR sources on the black body at all wavelengths, for collecting angles ranging from about 10 to 50 mrad. For larger angles (i.e., 100 mrad) the gain is reduced for both rings due to larger geometrical contributions to the source area. When comparing the two sources with each other, we see that the NSLS BM is more brilliant at short λ, due to the smaller value of its source size. In the case of DAΦNE, considering a definite front end with a slit limiting the collecting angle to 50 mrad in vertical, the ABR will be strongly modified at longer wavelength (see Fig. 5). Still the gain is very large in the mid IR and demonstrate the advantage of SR over a conventianal IR source.

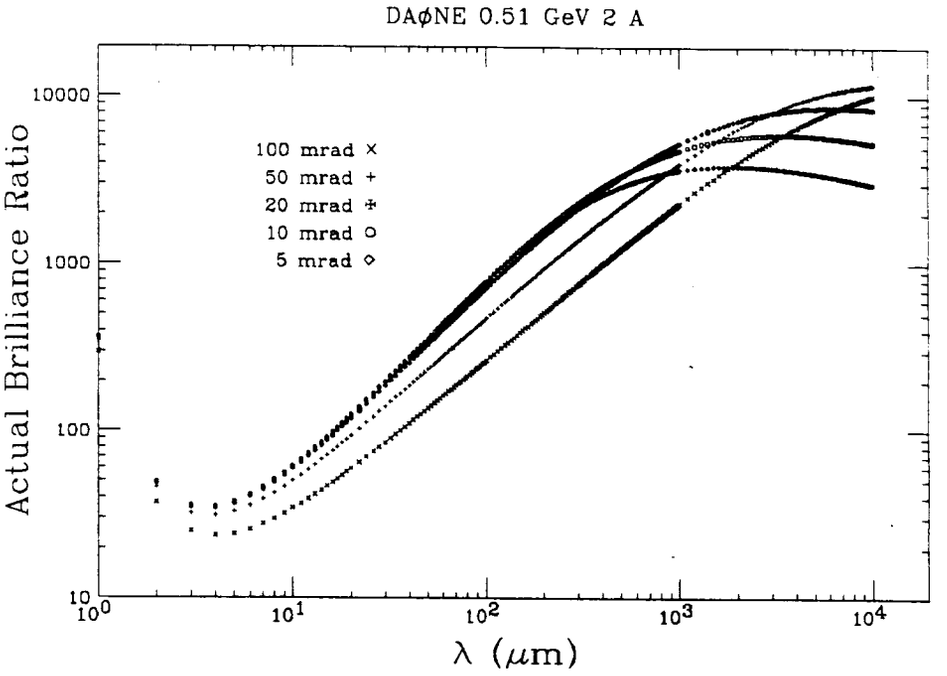

FIG. 3 – The ABR function of the DAΦNE source, as calculated for several values of the collecting angle θ.

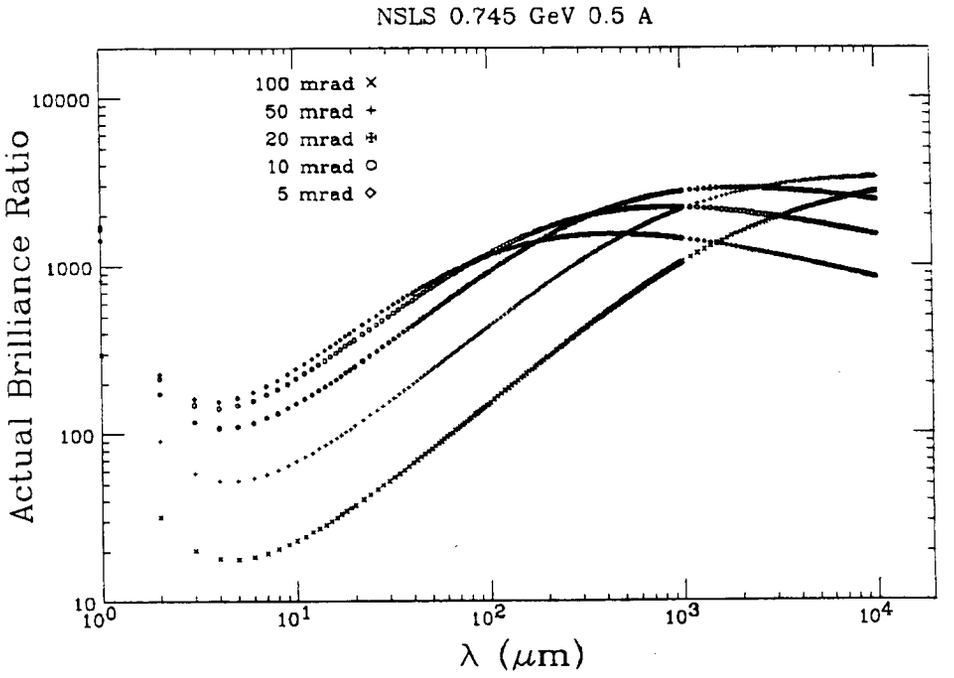

FIG. 4 – The ABR function of the NSLS source, as calculated for several values of the collecting angle θ.

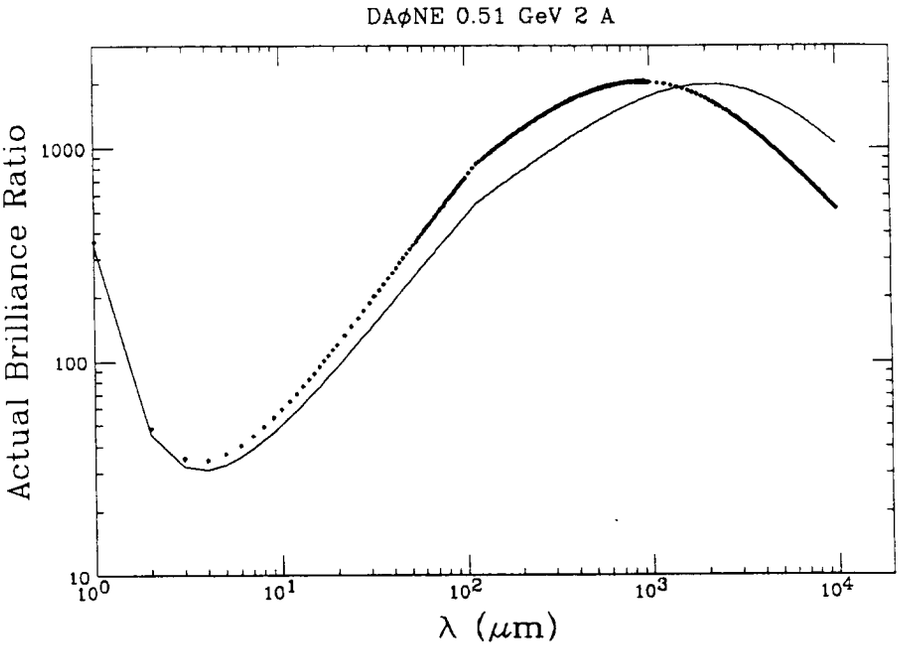

FIG. 5 – The "real" ABR function for a DAΦNE BM. The exit port is placed at 1200 mm from the source and limits the vertical collecting angle to 50 mrad. The solid line corresponds to 50 mrad horizontal collecting angle, the dotted one to 20 mrad.

APPENDIX

To estimate the horizontal and vertical geometrical broadening, we started from the definition of uniform distribution of charged particles along the trajectory in the BM. Being n_t the number of the particles in the bunch and L= ρθ/2 the half-length of the trajectory, we define the particle distribution function as $f = n_t/L$ (see Fig. 6). The average displacement along x may be evaluated by using the classical formula for the statistical average with a distribution f

$$< x > = \int_0^L d\ell x(\ell) f \Big/ \int_0^L d\ell f \qquad \text{(A1)}$$

where

$$x(\ell) = \rho\left[1-\cos\left(\frac{\ell}{\rho}\right)\right] \qquad \text{(A2)}$$

and the integral is performed along the arc $0 \le \ell \le L$. The r.m.s. displacement is defined as $\left(\sigma_x^{geo}\right)^2 = \langle x^2 \rangle - \langle x \rangle^2$, and it can be easily evaluated by using the following expressions for the first and the second moment of the variable x:

$$\langle x \rangle = \rho\left(1 - \frac{\sin\theta/2}{\theta/2}\right) \qquad \text{(A3)}$$

$$\langle x^2 \rangle = \frac{3}{2}\rho^2 + \frac{1}{2}\rho^2\frac{\sin\theta}{\theta} - 2\rho^2\frac{\sin\theta/2}{\theta/2} \qquad \text{(A4)}$$

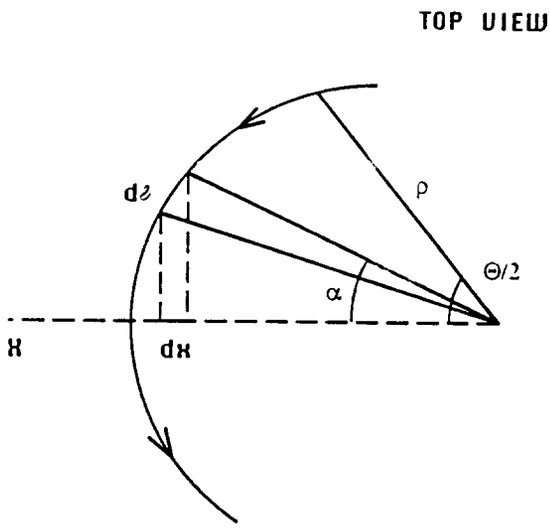

FIG. 6 – Top view of the beam trajectory in the bending magnet. The angle α indicates the position of the small portion dl of the trajectory arc. dx is the projection of dl on the x axis.

The above expressions allow the calculation of σ^{geo}_x for any ρ and θ values. However, the horizontal broadening σ^{geo}_x can be evaluated also in a different way. Indeed, a small length $d\ell$ of the trajectory is seen on the xy plane (defined in the text) as a small portion of source of

length dx (see Fig. 6). The number n of the source points seen in a small segment dx is given by $n = g(x)dx = f d\ell$ and the distribution g(x) is then defined by the relation

$$g(x) = f \left|\frac{d\ell}{dx}\right|$$

Being

$$\left|\frac{d\ell}{dx}\right| = \rho \frac{d\alpha}{dx} = \frac{1}{\sqrt{1-(1-x/\rho)}}$$

the particle distribution g(x) on the xy plane can be obtained. By using the distribution g(x) and considering the distribution f constant, the new value of the average x coordinate can be written as

$$\langle x \rangle = \rho\left(1 - \frac{\sin\theta/2}{\pi/2 - \arcsin(\cos\theta/2)}\right) \qquad \text{(A5)}$$

while the second moment of the distribution holds

$$\langle x^2 \rangle = \frac{3}{2}\rho^2 + \frac{1}{2}\rho^2 \sin\theta/2 \frac{(\cos\theta/2 - 4)}{\pi/2 - \arcsin(\cos\theta/2)} \qquad \text{(A6)}$$

It can be shown that Eqs. A5 and A6 coincide with the previous Eqs. A3 and A4 respectively, in the limit of small θ.

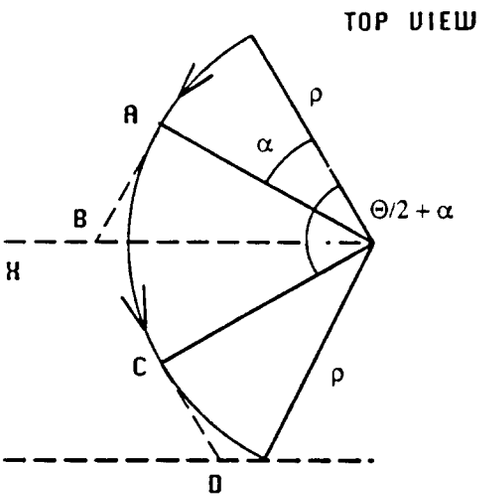

FIG. 7 – Top view of the geometry of the vertical broadening. The particles individuated by an angle α irradiate in a cone whose axis is along line AB. The broadening for such particles is determined by the length of AB. The particles at α+θ/2 irradiate in a cone with its axis along CD. The contribution to the vertical broadening is also proportional to the length of CD.

For the vertical contribution σ^{geo}_y the calculation is more complicated. To describe the vertical broadening, we have to distinguish among the particles which are placed before the xy source plane, and those that have already crossed that plane, shown in Fig. 7. Particles

placed before the xy plane, due to the large intrinsical divergence σ_ψ of the IR light, strongly contribute to the vertical dimension. However, such contribution decreases as the particles approach the xy plane. The source points placed after the xy plane give a smaller contribution, because their distance grows along the path and smears the effect associated with the opening angle of the radiation. In order to find the algebrical expression that describes the vertical broadening, we have to calculate the maximum vertical coordinate $y(\lambda,\alpha)_{max}$ for a photon impinging on the xy plane. This coordinate corresponds to the maximum size of the illuminated area in the source plane. Along the trajectory, any source point is individuated by an angle α (see Fig. 7). For $0 \le \alpha \le \theta/2$

$$y(\alpha,\lambda) = \rho \tan(\sigma_\psi/2) \tan[\theta/2 - \alpha] \qquad (A7)$$

while for $\theta/2 \le \alpha \le \theta$ the function $y(\alpha,\lambda)_{max}$ is

$$y(\alpha,\lambda) = \rho \tan(\sigma_\psi/2)\left[\frac{\sin\theta/2}{\sin(\pi/2 - \alpha + \theta/2)} - \tan(\alpha - \theta/2)\right] \qquad (A8)$$

Clearly, the vertical broadening depends on λ through σ_ψ. Equation A8 has been deduced for source points placed in front of the xy plane and their vertical distances $y(\lambda,\alpha)$ are calculated considering the distance between the emitting point and the end of the trajectory in the bending magnet (line CD in Fig. 7). As in the previous calculation for the horizontal broadening, we have evaluated the r.m.s. maximum vertical size associated to the uniform distribution f of the particles in the beam. In this case we have to consider that the number $n = f d\ell$ of particles in a small segment of trajectory emitting on the y>0 (or y<0) direction is only half of the total. The average values is then given by

$$\langle y^2 \rangle = \frac{1}{2}\int_0^L d\ell\, y^2(\ell) f \Big/ \int_0^L d\ell f \qquad (A9)$$

The above equation yields to

$$\langle y^2 \rangle = \rho^2 \frac{\tan^2(\sigma_\psi/2)}{2\theta}\left[\sin^2(\theta/2)\tan(\theta/2) - \theta + 2\sin(\theta/2)\right] \qquad (A10)$$

Because of the particular symmetry of the orbit, we considered only half of the whole trajectory in the calculation of the horizontal size. On the contrary, this short-cut is not allowed in the vertical case, because the rear and the front half of the beam give different contributions to the broadening. On the other hand the symmetry of the source emission yields to $\langle y \rangle = 0$ for an observer on axes.

The two geometrical contributions has been calculated neglecting the vertical and horizontal dimensions of the beam, which became negligible when large collection angles are considered. This approximation is satisfactorily verified because the formulas A3, A4 and

A10 depend on the orbital radius ρ, via a moltiplicative factor. As a consequence a wide electron beam can be virtually described as a change of the radius of the order of the horizontal size σ_{x0}, (usually <1 mm). It determines a relative variation of the calculated values of the order $\sigma_{x0}/\rho \approx 10^{-3}$.

Acknowledgments

The authors wish to thanks R. Cöisson and P. Roy for useful discussions.

References

1 V. Montelanici, LNF Internal Notes, LNF-72/56.
2 S.L. Hulbert and J.M. Weber, Nucl. Instr. Meth. A319, 25 (1992).
3 M.E. Biagini, C. Biscari, S. Guiducci, J. Lu, M.R. Masullo and G. Vignola, DAΦNE Technical Note L-9 (1993).
4 *"Synchrotron Radiation and Free Electron Lasers"*, CERN Accelerator School (Chester, 1989) CERN 90-03.
5 M. Bassetti, M.E. Biagini, C. Biscari, S. Guiducci, M.R. Masullo and G. Vignola, DAΦNE Technical Note L-1 (1991); DAΦNE Machine Project, LNF-92/033 (P) 1992
6 J. Murphy, Synchrotron Light Source Data Book, BNL 42333 (1990).
7 "X-Ray Data Booklet", Center for x-ray optics, Lawrence Berkeley Laboratory, University of California.
8 W.D. Duncan and G.P. Williams, Appl. Opt. 22, 2914 (1983).
9 G.P. Williams, Nucl. Instr. Meth. 195, 383 (1982).
10 S. Krinsky, M. Perlman and R.E. Watson, in: *'Handbook on Synchrotron Radiation'*, Ed. E.E. Koch, Vol. 1, Chapt. 2 (North Holland, 1983).
11 R. Cöisson, J. Phys. 45, L-89 (1984).
12 G. K. Green, *Spectra and Optics of Synchrotron Radiation*, BNL 50522, 1976.
13 V. O. Kostroun, Nucl. Instr. Meth. 172, 371 (1980).
14 M. Conversi (unpublished).